



## Research article

# ON donor tethered copper (II) and vanadium (V) complexes as efficacious anti-TB and anti-fungal agents with spectroscopic approached HSA interactions<sup>☆</sup>

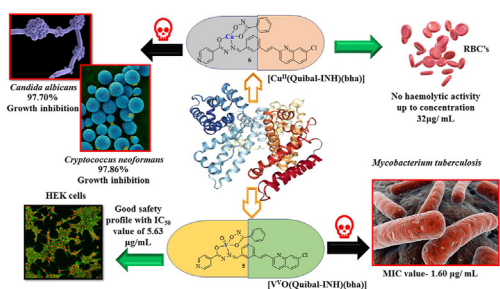


Anamika Sinha<sup>a,1</sup>, Riya Chaudhary<sup>a,1</sup>, Dinesh S. Reddy<sup>a,\*\*</sup>, Manasa Kongot<sup>a</sup>, Mahantesh M. Kurjogi<sup>b</sup>, Amit Kumar<sup>a,\*</sup>

<sup>a</sup> Centre for Nano and Material Sciences, Jain University, Jain Global Campus, Bengaluru, 562112, Karnataka, India

<sup>b</sup> Multi-Disciplinary Research Unit, Karnataka Institute of Medical Sciences, Hubli, India

## GRAPHICAL ABSTRACT



## ARTICLE INFO

## Keywords:

Drug resistance  
*Candida albicans*  
*Cryptococcus neoformans*,  
 Hemolysis  
 Free-radical scavenging  
 Spectroscopic technique

## ABSTRACT

Antimicrobial drug resistance poses a significant threat worldwide, hence triggering an urgent situation for developing feasible drugs. 3D-transition metal coordination complexes being multifaceted, offer tremendous potency as drug candidates. However, there are fewer reports on non-toxic and safe transition metal complexes; therefore, we hereby attempted to develop novel copper and vanadium-based therapeutic agents. We have synthesised six metal complexes viz., [V<sup>V</sup>O<sub>2</sub>(Quibal-INH)] (1), [Cu<sup>II</sup>(Quibal-INH)<sub>2</sub>] (2), [V<sup>V</sup>O(Quibal-INH) (cat)] (3), [Cu<sup>II</sup>(Quibal-INH) (cat)] (4), [V<sup>V</sup>O(Quibal-INH) (bha)] (5) and [Cu<sup>II</sup>(Quibal-INH) (bha)] (6). Quibal-INH (L) is an ON bidentate donor ligand synthesized from Schiff base reaction between 4-(2-(7-chloroquinolin-3-yl)vinyl) benzaldehyde (Quibal) and Isoniazid (INH). The synthesized compounds were characterized using analytical techniques involving ATR-IR, UV-Vis, EPR, <sup>1</sup>H NMR, <sup>13</sup>C NMR, and <sup>51</sup>V NMR. Ligand (L) and compound 3 exhibited moderate growth inhibitory activity towards *Candida albicans* and *Cryptococcus neoformans* fungal species. Compound 6 has been identified as active against the above fungal species with no toxicity and hemolysis activity on the healthy cells. Compound 5 exhibited significant activity against the *Mycobacterium tuberculosis*

<sup>☆</sup> This article is a part of the “Coordination compounds” Special issue.

\* Corresponding author.

\*\* Corresponding author.

E-mail addresses: [reddy.dinesh@jainuniversity.ac.in](mailto:reddy.dinesh@jainuniversity.ac.in) (D.S. Reddy), [amit.kumar@jainuniversity.ac.in](mailto:amit.kumar@jainuniversity.ac.in) (A. Kumar).

<sup>1</sup> Authors have contributed equally.

<https://doi.org/10.1016/j.heliyon.2022.e10125>

Received 1 June 2022; Received in revised form 12 July 2022; Accepted 27 July 2022

2405-8440/© 2022 The Author(s). Published by Elsevier Ltd. This is an open access article under the CC BY-NC-ND license (<http://creativecommons.org/licenses/by-nc-nd/4.0/>).

*H<sub>37</sub>R<sub>v</sub>* strain. Further, compounds 4, 5 and 6 exhibited excellent free radical scavenging activity. All the developed compounds were found to exhibit stability over a wide range of pH conditions. The complexes were additionally studied for their interaction with human serum albumin (HSA) with the UV-vis spectroscopic technique.

## 1. Introduction

Drug resistivity menace stimulated by the increased use and misuse of antimicrobials is one of the top 10 global threats to modern medicine and humanity according to the World Health Organisation (WHO) [1]. In addition, antimicrobial resistance and bacterial infections such as tuberculosis trigger prolonged illness and mortality [2a, 2b]. Amidst the COVID-19 pandemic, one of the most promising approaches for combating such outbreaks is designing therapeutic strategies and new drugs [3a]. Earlier, clinically approved compounds used for different diseases have been tested for SARS-Cov 2, wherein metal-based drugs like Auranofin, an FDA-approved gold-based drug for rheumatoid arthritis and works via immune modulation, are good candidates [2, 3]. The use of transition metals as therapeutic agents has become more pronounced over the past few decades. The development of cis-platin in the mid-19<sup>th</sup> century for cancer treatment revolutionized the field of transition metal chemistry [4, 5]. In the wake of this, other platinum-containing complexes like carboplatin [6] and oxoplatin [7] were also explored for more effectiveness and lower toxicity. This led to a major thrust in research activities involving other transition metal complexes as drug candidates as well, like Salvarsan (As-based) for the treatment of Syphilis, NAMI-A, and KP1019 (Ru-based) as anticancer drugs, BEOV and BMOV (V-based) for the treatment of diabetes [8, 9, 10].

One of the recent strategies is to develop metal complexes of known antibiotics or ligands possessing antimicrobial properties [11]. For example, 8-hydroxyquinolines (8HQ) are recognized for their antimicrobial properties and are present in numerous bioactive natural products. Several mixed ligands tethered metal complexes containing copper and vanadium 8HQ with picolinato, dipicolinato, and Schiff base were found to be very active against tuberculosis with MIC comparable to or better than the standard drug streptomycin [12]. Schiff bases have a host of industrial and catalytic uses and a plethora of biological functions. Additionally, they stabilize the metal ions, having variable oxidation states, by forming –N=CH– (azomethine) bonding from the lone pair of nitrogen, making them a potent pharmacophore [13]. In a recent study, novel macrocyclic Schiff base copper and vanadium complexes showed better antibacterial activity than the standard streptomycin against *Escherichia coli* [14]. Cu(II) complexes having formamidine-based dithiocarbamate ligands are active against most of the bacterial strains, but the ones with unsymmetrical ligand systems showed better antibacterial activity, while the complexes with symmetrical ligand systems showed better antioxidant activity with the lowest IC<sub>50</sub> value found to be  $1.10 \times 10^{-3}$  mM [15]. Amino thiophenol and formyl benzonitrile Schiff base appended Cu(II) complex exhibited significant growth inhibition against *Salmonella typhi* bacteria compared to the standard drug, chloramphenicol [16]. Cu-thiosemicarbazones have been explored as antimalarial, antifungal, and antibacterial agents. Isoniazid-related Cu(II) complexes were studied for their antimycobacterial activity against *M. tuberculosis* H<sub>37</sub>R<sub>v</sub>. The prepared complexes showed excellent inhibition with MIC values  $\leq 0.2$   $\mu\text{g/mL}$ . Cu(II) complexes of fluorinated isonicotinoylhydrazones exhibited significant activity against the single-drug-resistant *M. tuberculosis* strain [17, 18, 19]. Complexes of copper (II) coordinated with Schiff base derivatives containing benzofuran core displayed significant antibacterial activity with MIC values of 1.6  $\mu\text{g/mL}$  compared to the standards streptomycin (MIC = 6.25  $\mu\text{g/mL}$ ), pyrazinamide and ciprofloxacin (MIC = 3.12  $\mu\text{g/mL}$ ) against *M. Tuberculosis* [20]. Tetra-iodo salen Schiff base ligand-based copper complex showed better *E. coli* inhibition activity than the standard Ampicillin [21].

Several vanadium complexes have also been investigated as potent antimicrobial and antitubercular agents. The close resemblance of vanadate to phosphate with respect to their structure enables it to exhibit homologous behavior in the body [22]. V<sup>IV</sup>O-complexes with ciprofloxacin antibiotic and amino acid derivatives displayed better activity due to complexation against Gram-positive and negative bacteria. V<sup>IV</sup>O-complexes with ligand derived from the condensation of indoline-dione and phenyl-hydrazino thiadiazoles displayed higher antifungal activity against *C. pallescens*, *C. falcatum*, *A. niger*, and antibacterial activity against Gram-negative (*E. coli*, *Salmonella typhi*) and Gram-positive (*Staphylococcus aureus*, *Bacillus subtilis*) bacterial strains [23, 24]. V<sup>IV</sup>O and V<sup>V</sup> homoleptic complexes of 8HQ as well as heteroleptic complexes containing Schiff bases or picolinato molecules as co-ligands provided excellent results as therapeutics [12]. Chloro and bromo substituted hydrazone derived vanadium (V) complexes were studied as potential antimicrobial agents. The compounds showed comparable activity with respect to the standard penicillin G with MIC values ranging from 2.3–4.7  $\mu\text{g/mL}$  against *B. subtilis* and 4.7–9.4  $\mu\text{g/mL}$  against *S. aureus* [25]. Oxovanadium complexes with free thiosemicarbazone ligands showed good activity against *M. tuberculosis* with MIC values in the range of 62.5–1.56 ( $\mu\text{g/mL}$ ) [26].

Inspired by the numerous biologically active Schiff base appended copper and vanadium complexes, in the present work, a series of novel Cu(II) and V(V) complexes viz. [V<sup>VO</sup><sub>2</sub>(Quibal-INH)] (1), [Cu<sup>II</sup>(Quibal-INH)<sub>2</sub>] (2), [V<sup>VO</sup>O(Quibal-INH) (cat)] (3), [Cu<sup>II</sup>(Quibal-INH) (cat)] (4), [V<sup>VO</sup>O(Quibal-INH) (bha)] (5) and [Cu<sup>II</sup>(Quibal-INH) (bha)] (6) consisting of ON donor Schiff base ligand Quibal-INH (L) as primary ligand were synthesized (Figure-1). All the compounds were characterized, studied for their stability at physiological pH, and tested for their therapeutic potential as *in-vitro* antifungal, antibacterial, antitubercular, and antioxidant agents.

## 2. Experimental

### 2.1. Materials and instrumentation

All the reagents and chemicals used in this study were of analytical grade and used as purchased with no further purification carried out. [VO(acac)<sub>2</sub>], which is a vanadium (IV) precursor, was synthesized (see Supporting information Section 1.1) following a reported method [27]. Infrared spectrum in the range of 600–4000  $\text{cm}^{-1}$  was measured directly with an Eco-ATR-IR Bruker alpha spectrophotometer. Elemental analysis (CHN) was done on a Euro Vector E-3000 instrument. <sup>1</sup>H and <sup>13</sup>C-NMR spectra were measured in Agilent 400 MHz FT-NMR spectrometer in the presence of tetramethylsilane as the internal standard. <sup>51</sup>V-NMR spectra were obtained from Varian-Mercury Plus 300MHz NMR spectrometer using ammonium vanadate as the internal standard. UV-Visible spectra were measured with a Shimadzu UV-1800 Spectrophotometer. X-band solution EPR spectra were obtained under liquid nitrogen temperature conditions from a JES-FA200 JEOL ESR Spectrometer. The pH of solutions was measured using Hannah HI-5000 pH meter, which was calibrated with pH 4–7 standard buffers.

### 2.2. Antimicrobial activity, haemolytic activity, and cytotoxicity activity studies

Primary antimicrobial testing was accomplished via growth inhibition assay using the test compounds at a single concentration, in duplicate (see Supporting information Section 1.2). Growth inhibition percents were measured for four Gram-negative bacteria: *Acinetobacter*

*baumannii* (Ab), *Klebsiella pneumonia* (Kp), *Pseudomonas aeruginosa* (Pa), *Escherichia coli* (Ec); one Gram-positive bacteria: *Staphylococcus aureus* (Sa) and two fungi: *Cryptococcus neoformans* (Cn) and *Candida albicans* (Ca). Samples were dissolved in DMSO and water to obtain the required concentration of 32 µg/mL or 20 µM for testing in a 384-well, non-binding surface plate for the pathogenic strain, fixing the DMSO concentration to a maximum of 1%. Samples are categorized as hits if the growth inhibition value is ≥80%. Samples are partial hits if the growth inhibition value is in the range of 50.9%–79.9% [28].

### 2.3. Antitubercular assay

The antitubercular testing was performed using Microplate Alamar Blue assay (MABA) against *M. tuberculosis*. In brief, a sterile 96-well plate added with Middlebrook 7H9 broth (100 µL) was used for testing. The compounds were serially diluted directly on the plate, and the final test drug concentrations used were 100 to 0.2 µg/mL. Consequently, plates were incubated at 37 °C for five days. Following incubation, 25µL of 1:1 freshly prepared mixture of Tween 80 (10%) and Alamar Blue reagent were added to the plate and incubated for 24 h. An intact blue color indicated the absence of any bacterial growth, and pink color suggested bacterial growth in the well. The MIC values were then calculated, indicating the lowest drug concentration that prevented any blue to pink color change [29a].

### 2.4. In-vitro cytotoxicity assay

HEK-293 cells were trypsinized and aspirated for the toxicity studies, and the cell pellet was prepared by centrifugation. Cell suspension (200µL) was added to a 96-well plate and incubated at 37 °C and a 5% CO<sub>2</sub> atmosphere for 24 h. 200µL of different test concentrations (0.15, 0.75, 1.5, 3, and 6 µg/mL from stock) of the compounds were added to the respective wells. The plate was again incubated in the same way as before. Subsequently, 100µL of media containing MTT reagent (10%) was added to each well, followed by incubation for 3 h. The culture medium was then completely removed without disturbing the formed crystals. DMSO (100µL) was added to solubilize the crystals of formazan. The absorbance was measured using a microplate reader at 570 nm and 630 nm. The growth inhibition percentage was calculated using the absorbance values, and the concentration of test compounds required to prevent cell growth by 50% (IC<sub>50</sub>) was evaluated from the dose-response curves [29b, 29c].

### 2.5. Free-radical scavenging assay

The free-radical scavenging ability of the compounds was evaluated with the help of 2,2-diphenyl-1-picrylhydrazyl (DPPH) radical scavenging assay [30]. For this assay, a stock solution of all compounds (1 mg/mL) was prepared in DMSO, and this was further diluted serially to final concentrations of 1, 2, 3, 4, 5, 10, 20, 50, 80, and 100 µg/mL. The stock solution of DPPH (10 mL, 1 mM) was prepared in methanol and further diluted (25 mL, 0.1 mM) for use in the radical scavenging experiments. Equal volumes (1 mL each) of diluted DPPH and compound solutions were mixed in glass vials, shaken well, and kept for 30 min at room temperature before measuring the absorbance. The absorbance of all solutions of DPPH titrated with various compound concentrations was measured using a UV-Vis spectrophotometer at 517 nm. Ascorbic acid was used as a standard antioxidant reference for this assay.

DPPH radical scavenging percentage of the compounds was calculated using Eq. (1).

$$\frac{(A_0 - A)}{A_0} \times 100 = \% \text{ Scavenging effect} \quad 1$$

Where A<sub>0</sub> is the absorbance of blank (DMSO + DPPH solution), and A is the absorbance of sample mixtures added with DPPH.

## 2.6. Solution stability studies

### 2.6.1. Titration experiments at varied pH

For the titration experiments at varied pH conditions [31], a pH meter and UV-Vis spectrometer were used. Solution of the complexes (0.5 mM, 50 mL) were prepared in water and DMSO solvent media. Standard solutions of HCl (50 mM, 100 mL) and KOH (50 mM, 100 mL) were prepared in water. The pH of the sample solution was varied in the 3–9 pH range. The same protocol was followed for UV-Vis spectroscopic titration. Graph of absorbance v/s wavelength was plotted to determine the behavior of the complexes in acidic and basic media.

### 2.7. Interaction with serum protein HSA

A successful drug development program requires an analysis of the interactions between drug candidates and carrier proteins such as human serum albumins (HSA) [31c, 32, 33]. This study will help in understanding the pharmacodynamics and pharmacokinetics of the binding components and thus gain insight into the structural changes that are induced by drugs on their carriers [31, 32, 33, 34, 35]. Hence, the interaction behaviour of the complexes with carrier protein human serum albumin (HSA) was studied. For this, stock solution of all the compounds (0.1 mM in DMSO) were prepared. HSA standard solution (5 µM) was prepared in a 7.4 pH buffer of sodium phosphate [32]. The interaction was studied using a UV-Vis spectrophotometer. For the titration experiments, the HSA concentration used was 5 µM and 0–10 µM concentration of the test compounds were consecutively used to evaluate the change in absorbance.

## 2.8. Synthetic methodology

### 2.8.1. Synthesis of N'-(3-(2-(7-chloroquinolin-3-yl)vinyl)benzylidene)isonicotinohydrazide, Quibal-INH (L)

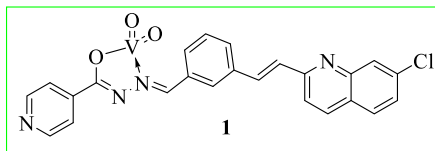
3-(2-(7-chloroquinolin-3-yl)vinyl)benzaldehyde (Quibal) (4.00 g, 6.80 mM) was dissolved in DCM. Isoniazid (INH) (1.86 g, 6.80 mM) was taken in ethanol and sonicated for proper dissolution. The two starting materials were mixed, and this solution mixture was refluxed for 3 h. Cream-coloured solid precipitated out, and upon reaction completion, the product was filtered and washed using DCM to remove unreacted quinoline aldehyde, if any. The obtained residue was dried at 60 °C and further used to synthesize complexes. The ligand was structurally characterized, and these results were found to match the ligand's predicted structure. Yield: 3.92 g, 69.70%; Anal. calcd. for. C<sub>24</sub>H<sub>17</sub>N<sub>4</sub>OCl (MW: 412.87 g mol<sup>-1</sup>): C, 67.22; H, 5.45; N, 13.07. Found: C, 67.21; H, 5.38; N, 12.78; Selected IR data (cm<sup>-1</sup>/ν<sub>str</sub>): 3394 (N–H), 3020 (Aromatic C–H), 2839 (aliphatic C–H), 1648 (C=O), 1604 (C=N), 1549 (ring C=N), 1308 (C–N), 1065 (C–C); <sup>1</sup>H-NMR (DMSO-d<sub>6</sub>, ppm): 8.81–7.55 (m, 13H, aromatic H), 8.53 (s, 1H, N=CH), 7.54 (m, 2H, -CH = CH); <sup>13</sup>C-NMR (DMSO-d<sub>6</sub>, ppm): 162.16, 157.11, 150.78, 149.04, 148.48, 140.92, 137.18, 137.08, 135.19, 134.80, 130.23, 129.92–129.38 (4C), 127.90, 127.71, 127.21, 126.73, 126.12, 121.99, 120.81 (2C).

### 2.8.2. Synthesis of primary ligand complexes of vanadium and copper, [V<sup>V</sup>O<sub>2</sub>(Quibal-INH)] (1) and [Cu<sup>II</sup>(Quibal-INH)<sub>2</sub>] (2)

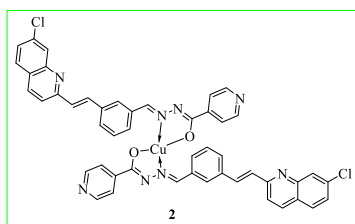
Vanadyl acetylacetonate (0.70 g, 2.66 mM) and copper chloride dihydrate (0.45 g, 2.66 mM) were dissolved separately in a minimum amount of methanol, and to these, a solution of ligand L (1.00 g, 2.42 mM) dissolved in a mixture of DCM and methanol in the ratio of 1:1 (60 mL) was added. The above two solutions were refluxed for around 3 h. Yellowish green colored and light green colored precipitates were obtained, respectively. The precipitates were separated through filtration, washed with methanol and DCM mixture, and dried in a vacuum to obtain the oxidovanadium(V) complex 1 and copper (II) complex 2 respectively.

**V<sup>V</sup>O<sub>2</sub>(Quibal-INH)] (1):** Yield: 0.74 g, 56.30 %; Anal. calcd. for. C<sub>24</sub>H<sub>16</sub>ClN<sub>4</sub>O<sub>3</sub>V (MW: 494.80 g mol<sup>-1</sup>): C, 52.30; H, 4.25; N, 7.87.

Found: C, 53.03; H, 4.23; N, 8.63; Selected IR data ( $\text{cm}^{-1}/\nu_{\text{str}}$ ): 3050–3170 (Aromatic C–H), 2833 (aliphatic C–H), 1598 (C=N), 1521 (ring C=N), 1322 (C–N), 1143 (C–O), 1075 (C–C), 965 (V=O);  $^1\text{H-NMR}$  (DMSO- $d_6$ , ppm): 8.36–7.62 (m, 13H, aromatic H), 8.76 (s, 1H, N=CH), 7.53 (m, 2H, -CH = CH);  $^{13}\text{C-NMR}$  (DMSO- $d_6$ , ppm): 172.34, 156.99, 156.83, 149.06, 148.37, 136.96, 135.10, 134.71, 130.23, 130.10, 129.80, 129.54, 129.28, 127.62, 127.12, 126.63, 126.02, 121.94, 120.72;  $^{51}\text{V-NMR}$  (DMSO- $d_6$ , ppm): -499.42.



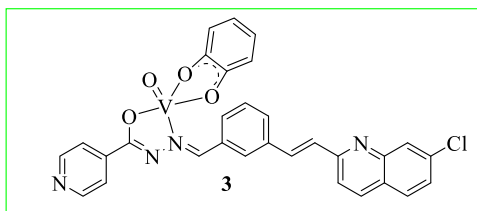
**[Cu<sup>II</sup>(Quibal-INH)<sub>2</sub>] (2):** Yield: 1.57 g, 66.89%; Anal. calcd. for. C<sub>48</sub>H<sub>32</sub>Cl<sub>2</sub>CuN<sub>5</sub>O<sub>3</sub>(MW: 887.27 g mol<sup>-1</sup>): C, 43.10; H, 2.48; N, 6.75. Found: C, 43.72; H, 3.46; N, 6.83; Selected IR data ( $\text{cm}^{-1}/\nu_{\text{str}}$ ): 2995 (Aromatic C–H), 2886 (aliphatic C–H), 1596 (C=N), 1524 (ring C=N), 1324 (C–N), 1154 (C–O), 1062 (C–C).



### 2.8.3. Synthesis of secondary ligand complexes of vanadium and copper, [V<sup>V</sup>O(Quibal-INH)(cat)] (3), [Cu<sup>II</sup>(Quibal-INH)(cat)] (4), [V<sup>V</sup>O(Quibal-INH)(bha)] (5) and [Cu<sup>II</sup>(Quibal-INH)(bha)] (6)

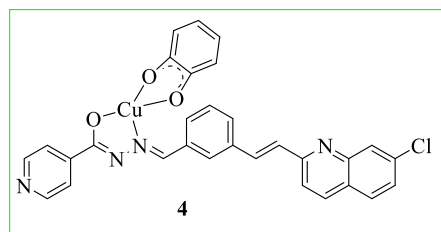
Vanadyl acetylacetonate (0.70 g, 2.66 mM) and copper chloride dihydrate (0.45 g, 2.66 mM) were dissolved separately in least amount of methanol, and to these, a solution of ligand L (1.00 g, 2.42 mM) dissolved in a mixture of DCM and methanol in the ratio of 1:1 (60 mL) was added. The above two solutions were refluxed for 30 min. Subsequently, catechol/benzohydroxamic acid (2.42 mM) was dissolved in 20 mL methanol and was added to the reaction mixtures, followed by refluxing for another 4 h. The precipitates were separated by filtration, washed, and dried to obtain dark green colored precipitates of vanadium compounds 3 and 5 and bottle green colored precipitates of copper compounds 4 and 6.

**[V<sup>V</sup>O(Quibal-INH)(cat)] (3):** Yield: 1.41 g, 78.97 %; Anal. Calcd. for. C<sub>30</sub>H<sub>20</sub>ClN<sub>4</sub>O<sub>4</sub>V (MW: 586.90 g mol<sup>-1</sup>): C, 55.94; H, 4.69; N, 8.16. Found: C, 56.15; H, 4.19; N, 7.50; Selected IR data ( $\text{cm}^{-1}/\nu_{\text{str}}$ ): 3044–3198 (Aromatic C–H), 2980 (aliphatic C–H), 1597 (C=N), 1548 (ring C=N), 1309 (C–N), 1144 (C–O), 1061 (C–C), 967 (V=O);  $^1\text{H-NMR}$  (DMSO- $d_6$ , ppm): 6.59–8.40 (m, 17 aromatic hydrogens), 8.81 (s, 1H, N=CH), 7.57 (m, 2H, -CH = CH);  $^{13}\text{C-NMR}$  (DMSO- $d_6$ , ppm): 172.43, 157.06, 156.85, 150.76, 149.07, 148.43, 140.99, 137.18, 137.12, 135.14, 134.78, 130.21, 129.90, 129.66, 129.51, 129.37, 127.67, 127.20, 126.73, 126.09, 121.98, 120.77.  $^{51}\text{V-NMR}$  (DMSO- $d_6$ , ppm): -506.16.

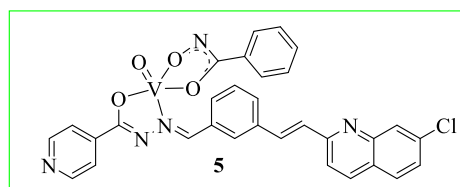


**[Cu<sup>II</sup>(Quibal-INH)(cat)] (4):** Yield: 1.01 g, 57.34%; Anal. Calcd. for. C<sub>30</sub>H<sub>20</sub>ClCuN<sub>4</sub>O<sub>3</sub>(MW: 583.50 g mol<sup>-1</sup>): C, 51.67; H, 3.52; N, 6.51.

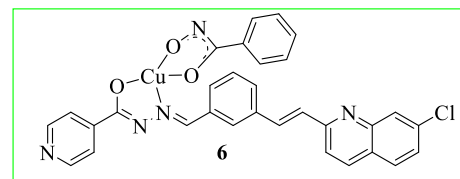
Found: C, 51.93; H, 3.51; N, 8.74; Selected IR data ( $\text{cm}^{-1}/\nu_{\text{str}}$ ): 3051 (Aromatic C–H), 2834 (aliphatic C–H), 1597 (C=N), 1521 (ring C=N), 1323 (C–N), 1155 (C–O), 1074 (C–C).



**[V<sup>V</sup>O(Quibal-INH)(bha)] (5):** Yield: 1.23 g, 72.13%; Anal. Calcd. for. C<sub>31</sub>H<sub>22</sub>ClN<sub>5</sub>O<sub>4</sub>V (MW: 614.93 g mol<sup>-1</sup>): C, 65.79; H, 4.10; N, 12.37. Found: C, 65.75; H, 5.12; N, 12.53; Selected IR data ( $\text{cm}^{-1}/\nu_{\text{str}}$ ): 3045–3205 (Aromatic C–H), 2841 (aliphatic C–H), 1595 (C=N), 1564 (ring C=N), 1306 (C–N), 1142 (C–O), 1061 (C–C), 965 (V=O);  $^1\text{H-NMR}$  (DMSO- $d_6$ , ppm): 8.81–7.53 (m, 18 aromatic hydrogens), 8.80 (s, 1H, N=CH), 7.51 (m, 2H, -CH = CH);  $^{13}\text{C-NMR}$  (DMSO- $d_6$ , ppm): 162.15, 157.06, 150.76, 150.00, 149.05, 148.45, 140.89, 137.15, 137.01, 135.16, 134.77, 130.18, 129.87, 129.63, 129.35, 127.89, 127.70, 127.19, 126.71, 126.08, 123.64, 121.99, 120.77.



**[Cu<sup>II</sup>(Quibal-INH)(bha)] (6):** Yield: 1.26 g, 74.91%; Anal. Calcd. for. C<sub>31</sub>H<sub>22</sub>ClCuN<sub>5</sub>O<sub>3</sub>(MW: 611.54 g mol<sup>-1</sup>): C, 60.00; H, 4.26; N, 10.76. Found: C, 61.49; H, 4.15; N, 10.05; Selected IR data ( $\text{cm}^{-1}/\nu_{\text{str}}$ ): 3058 (Aromatic C–H), 2841 (aliphatic C–H), 1596 (C=N), 1522 (ring C=N), 1322 (C–N), 1145 (C–O), 1076 (C–C).

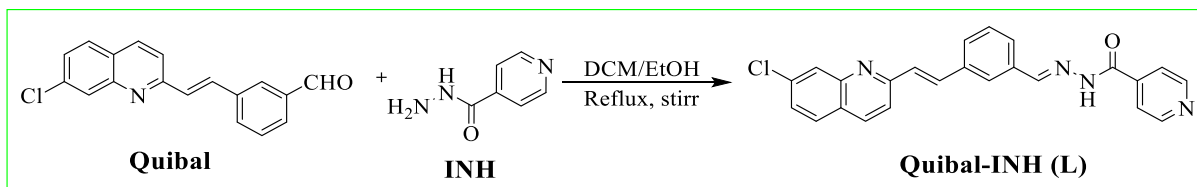


## 3. Results and discussion

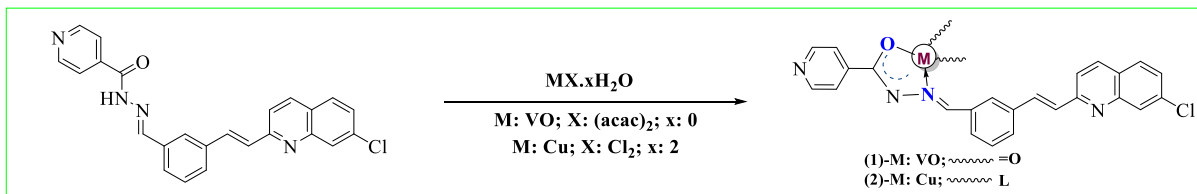
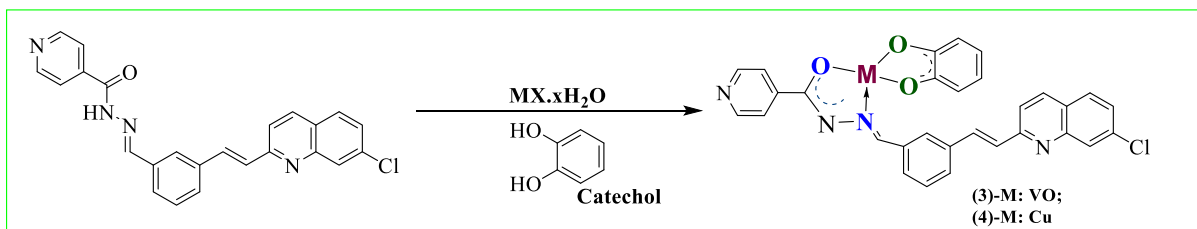
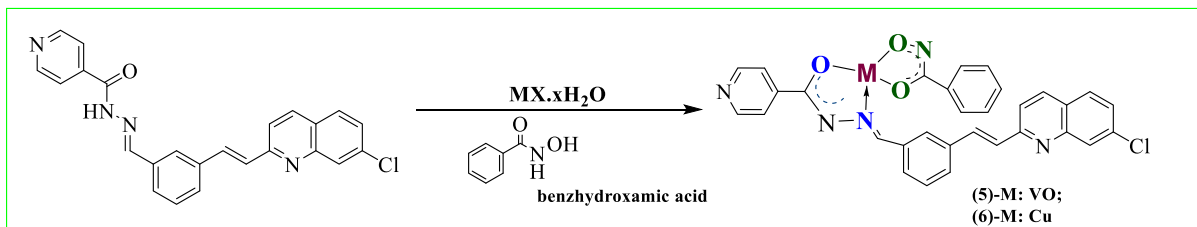
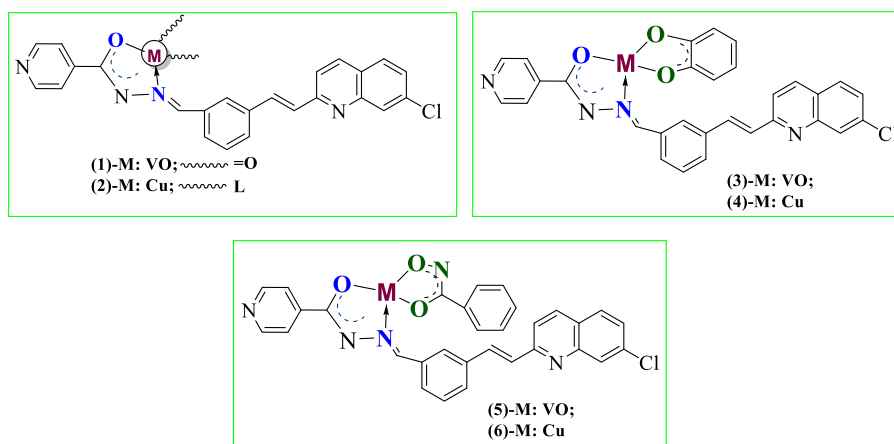
### 3.1. Synthesis and characterizations

Quibal-INH (L) was synthesized following a condensation reaction between a quinoline derivative (Quibal) and isoniazid (INH) (Scheme 1). Metal complexes (1 and 2) were synthesized following the reaction between the ligand and the corresponding metal precursor salts of copper and vanadium (Scheme 2). Further, four other complexes (3, 4, 5, and 6) were obtained with one unit of primary ligand, Quibal-INH, and another unit comprising secondary ligands, catechol (cat), and benzohydroxamic acid (bha) attached to the metal centre (Scheme 3 and Scheme 4). The ligand, as well as the metal complexes, were soluble in DMSO. The analytical data obtained for the compounds were found to be in full agreement with the proposed formulae of compounds.

$^1\text{H-NMR}$  analysis of L gave characteristic signals for 17 protons as predicted for the structure of the ligand (see Supporting information Figure 1a). The aromatic protons resonated between 8.81–7.55 ppm. The hydrogen atom associated with the carbon of the imine bond resonated at 8.53 ppm. The protons linked with the aliphatic double-bonded carbon atoms appeared at 7.54 ppm.  $^1\text{H-NMR}$  analysis of the vanadium (V)



Scheme 1. Synthesis route to obtain Quibal-INH(L).

Scheme 2. Synthesis route to obtain [VVO<sub>2</sub>(Quibal-INH)] (1) and [Cu<sup>II</sup>(Quibal-INH)<sub>2</sub>] (2).Scheme 3. Synthetic route employed to obtain [VVO(Quibal-INH) (cat)] (3), [Cu<sup>II</sup>(Quibal-INH) (cat)] (4).Scheme 4. Synthetic route employed to obtain [VVO(Quibal-INH) (bha)] (5) and [Cu<sup>II</sup>(Quibal-INH) (bha)] (6).

**Figure-1.** Structures of copper and vanadium metal complexes consisting of ligand Quibal-INH (L) as primary ligand were (1) represents [V<sup>VO</sup><sub>2</sub>(Quibal-INH)], (2) represents [Cu<sup>II</sup>(Quibal-INH)<sub>2</sub>], (3) represents [V<sup>VO</sup>O(Quibal-INH) (cat)], (4) represents [Cu<sup>II</sup>(Quibal-INH) (cat)], (5) represents [V<sup>VO</sup>O(Quibal-INH) (bha)] and (6) represents [Cu<sup>II</sup>(Quibal-INH) (bha)].

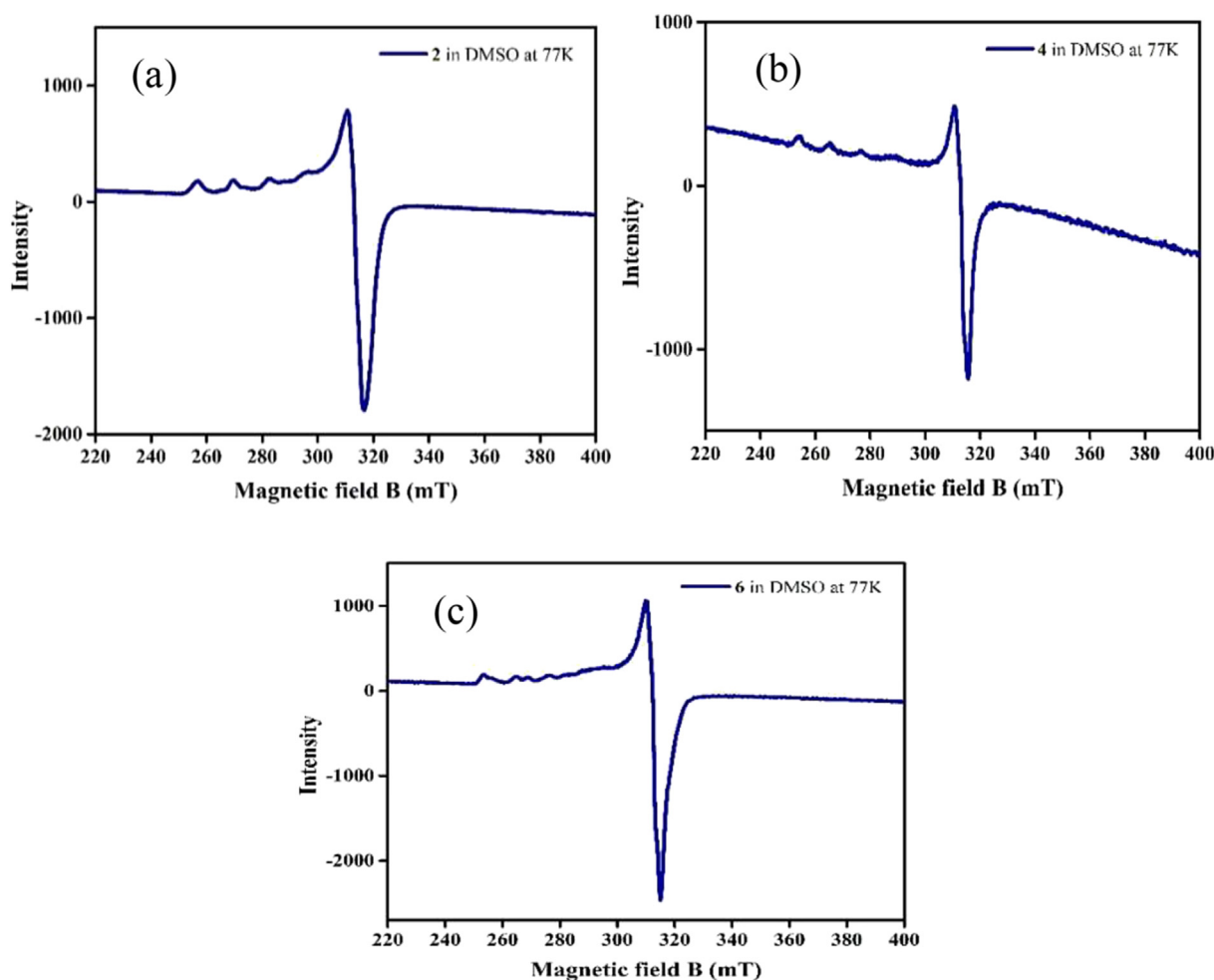


Figure-2. EPR spectra of (a)  $[\text{Cu}^{\text{II}}(\text{Quibal-INH})_2]$  (2), (b)  $[\text{Cu}^{\text{II}}(\text{Quibal-INH}) (\text{cat})]$  (4) and (c)  $[\text{Cu}^{\text{II}}(\text{Quibal-INH}) (\text{bha})]$  (6) in DMSO obtained at LNT (77 K).

Table 1. Spin-Hamiltonian parameters calculated using X-band EPR spectra of  $[\text{Cu}^{\text{II}}(\text{Quibal-INH})_2]$  (2),  $[\text{Cu}^{\text{II}}(\text{Quibal-INH}) (\text{cat})]$  (4) and  $[\text{Cu}^{\text{II}}(\text{Quibal-INH}) (\text{bha})]$  (6) in DMSO.

Sample	$g_x = g_y = g_{\perp}$	$g_z = g_{\parallel}$	$A_x = A_y = A_{\perp} (10^{-4} \text{ cm}^{-1})$	$A_z = A_{\parallel} (10^{-4} \text{ cm}^{-1})$	$g_{\parallel}/A_{\parallel} (\text{cm})$
2	2.08	2.35	101.45	145.95	161.01
4	2.08	2.39	98.94	129.87	184.03
6	2.08	2.38	116.02	141.18	168.58

Table 2. Growth inhibition values for high-risk pathogen species with the treatment of test compounds.

Sample (32 $\mu\text{g/mL}$ )	% of growth inhibition						
	Sa	Ec	Kp	Pa	Ab	Ca	Cn
L (Quibal-INH)	-	1.72	-	22.82	4.19	<b>50.18</b>	27.62
1	1.26	-	-	12.92	-	<b>48.48</b>	<b>49.13</b>
2	-	-	-	21.32	-	10.07	28.56
3	13.03	-	-	-	9.71	<b>48.55</b>	-
4	15.02	17.69	20.85	24.54	28.14	29.74	7.67
5	16.84	-	16.94	-	5.53	13.25	7.22
6	18.03	12.57	13.55	20.85	24.17	<b>97.70</b>	<b>97.86</b>

Sa: *Staphylococcus aureus*; Ec: *Escherichia coli*; Kp: *Klebsiella pneumoniae*; Ab: *Acinetobacter baumannii*; Pa: *Pseudomonas aeruginosa*; Ca: *Candida albicans*; Cn: *Cryptococcus neoformans*.

complexes (1, 3, and 5) showed minor changes in the resonant signals of the aromatic protons and the protons associated with the aliphatic double-bonded carbons (see Supporting information Figures 1b-1d). The hydrogen atom linked with the carbon of imine bond was observed to be de-shielded by 0.23 ppm, 0.28 ppm, and 0.27 ppm in 1, 3, and 5, respectively.  $^{13}\text{C-NMR}$  analysis of L showed expected signals for all the 24 carbons (see Supporting information Figure 2a). The signal at 162.16 ppm is due to carbonyl carbon and the imine carbon resonated at 149.04 ppm. All aromatic carbons resonated between 120.81-157.11 ppm. The  $^{13}\text{C-NMR}$  analysis of the complexes (1, 3, and 5) exhibited all resonance signals pertaining to the ligand. The carbon atom of imine was observed to be de-shielded by 7.79 ppm in 1, 23.39 ppm in 3, and 13.11 ppm in 5 (see Supporting information Figures 2b-2d). The formation of vanadium (V) complexes was further confirmed by performing a  $^{51}\text{V-NMR}$  spectral analysis. Compounds 1 and 3 exhibited a strong resonance at  $\delta = -499.42$  ppm and  $-506.16$  ppm, respectively, which confirms vanadium's

Table 3. MIC values of the compounds against  $H_37R_v$  strain.

Sample/drug	MIC value ( $\mu\text{g/mL}$ )
5	1.60
Streptomycin	0.80
Isoniazid	1.60
Rifampin	0.80
Ethambutol	3.20
Pyrazinamide	3.12

**Table 4.** EC<sub>50</sub> values of the compounds for free radical scavenging activity obtained from the DPPH radical scavenging study.

Sample	Ascorbic acid	L	1	2	3	4	5	6
EC <sub>50</sub> (μM)	66.42	-	672.94	146.20	106.09	18.33	48.66	72.55
EC <sub>50</sub> (μg/mL)	11.69	-NA-	332.97	129.72	62.26	10.69	29.92	44.37

oxidation state and supports the participation of the ON donor system for vanadium (V) coordination.

Copper (II) complexes (2, 4, and 6) were studied using EPR spectroscopy. The X-band EPR spectra of the copper complexes in DMSO solution ( $5 \times 10^{-4}$  M) were studied at liquid nitrogen temperature. The spectra displayed hyperfine signals characteristic of copper (II) metal centre. Manual stimulations were used to estimate g and A, the spin-Hamiltonian parameters (Table 1). These calculated hyperfine splitting constants could be equated to the ligands surrounding the copper center. All copper compounds exhibited an axial type of EPR spectrum ( $g_x = g_y < g_z$ ) (Figures 2a-c). The splitting constants were correlated with the  $g_{\parallel}/A_{\parallel}$  plots given by Peisach [36] and Addison [37], which provides the relation between geometry and  $g_{\parallel}/A_{\parallel}$  values. It was observed that the  $g_{\parallel}$  and  $A_{\parallel}$  values obtained are close to the predicted binding donor sets given in Peisach and Blumberg plot and Addison plot of  $A_{\parallel}$  vs  $g_{\parallel}$ . The tetrahedral distortion index values suggested a square planar arrangement around the central metal ion in a distorted environment.

I.R. spectra of the compounds provided evidence for the functional groups in all the compounds. The ligand (L) displayed a sharp band at  $1604 \text{ cm}^{-1}$  pertaining to the imine group ( $\text{C}=\text{N}$ ). The peak at  $3394 \text{ cm}^{-1}$  was due to the N-H stretching of the isoniazid moiety. No N-H peak was observed in the spectra of all the coordination compounds due to the loss

of amine hydrogen upon coordination to the metal center after the N-H and C=O groups in ligand exhibited tautomerism. The ligand peaks at  $1648 \text{ cm}^{-1}$  and  $1604 \text{ cm}^{-1}$  are associated with C=O and C=N stretching, respectively. The C=N peak underwent a significant shift, and the C=O peak vanished upon coordination of ligand with the metal centers indicating the contribution of enolic O and imino N as donor atoms in the metal complexes. Bands of medium intensity in the range of  $1549 \text{ cm}^{-1}$  to  $1065 \text{ cm}^{-1}$  were found due to ring C=N, C-N, and C-C stretching vibrations, which show negligible shifts in the metal complexes depicting that the ligand backbone is intact. Sharp bands at  $965 \text{ cm}^{-1}$ ,  $967 \text{ cm}^{-1}$  and  $965 \text{ cm}^{-1}$  were found for the metal complexes 1, 3 and 5, respectively, which pertain to V=O stretching modes.

### 3.2. Growth inhibition study against pathogens of high risk

Inhibition of growth of bacteria was examined by measuring the absorbance of samples at 600 nm (OD<sub>600</sub>). Inhibition of growth of fungi species was examined by determining the absorbance of samples at 530 nm and the absorbance difference between 600 and 570 nm (OD<sub>600-570</sub>), respectively. All synthesized compounds were found to be inactive towards growth inhibition of bacterial species in the primary screening assay (Table 2). However, the compounds exhibited moderate to

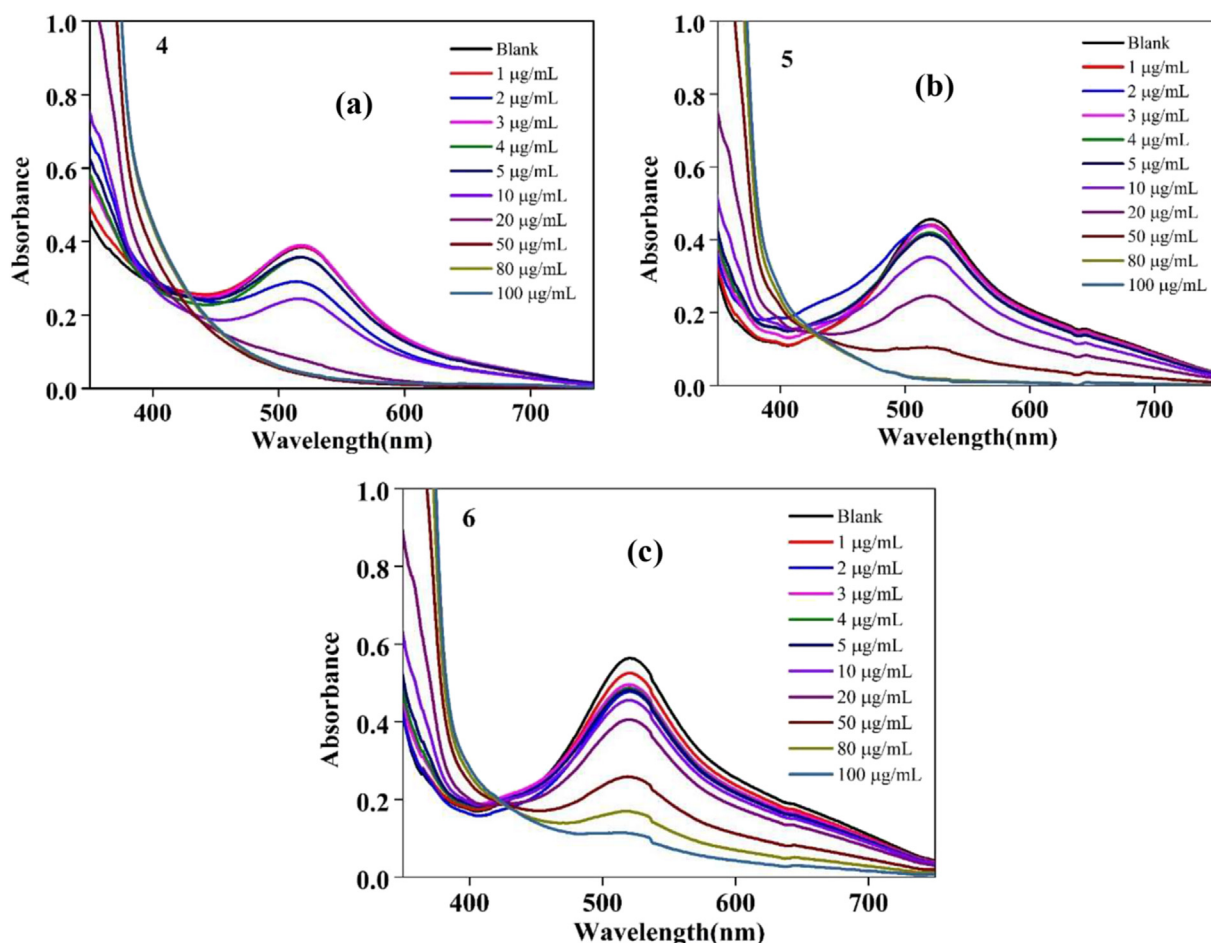


**Figure-3.** DPPH radical scavenging graphs of (a)  $[\text{Cu}^{\text{II}}(\text{Quibal-INH}) (\text{cat})]$  (4), (b)  $[\text{V}^{\text{V}}\text{O}(\text{Quibal-INH}) (\text{bha})]$  (5) and (c)  $[\text{Cu}^{\text{II}}(\text{Quibal-INH}) (\text{bha})]$  (6).

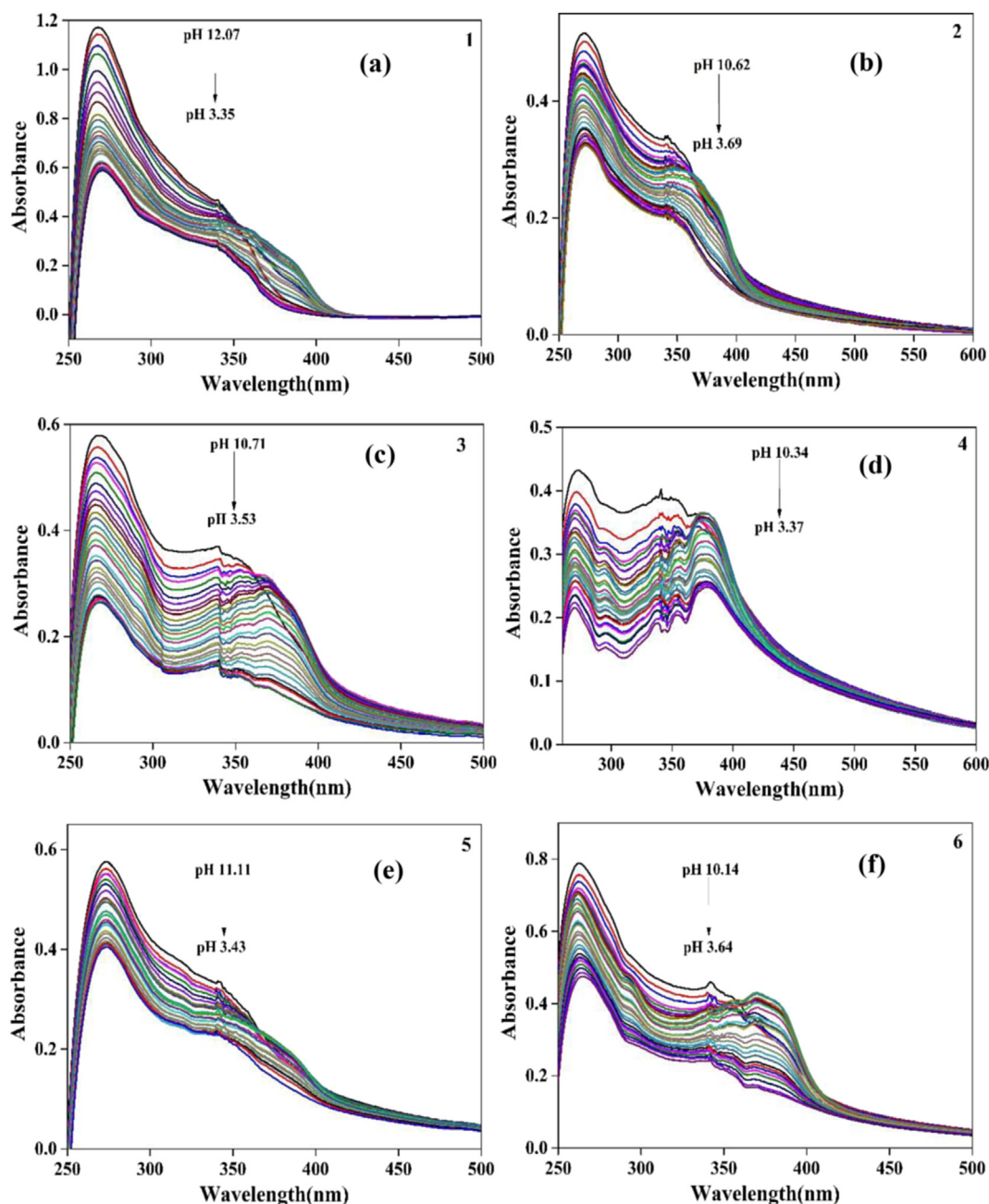


Figure-4. Plots obtained from UV-Visible pH titration studies of (a)  $V^{VO}_2(Quibal-INH)$  (1), (b)  $[Cu^{II}(Quibal-INH)_2]$  (2), (c)  $[V^{VO}(Quibal-INH) (cat)]$  (3), (d)  $[Cu^{II}(Quibal-INH) (cat)]$  (4), (e)  $[V^{VO}(Quibal-INH) (bha)]$  (5) and (f)  $[Cu^{II}(Quibal-INH) (bha)]$  (6).

excellent action against fungi pathogens. The copper complex (6) displayed significant inhibitory activity of 97.70% and 97.86% against *C. albicans* and *C. neoformans* fungi species, respectively. Thus, compound 6 has been identified as active and has been selected for further hit validation screening. This complex was further evaluated for its toxicity effect and haemolytic activity on human embryonic kidney cells and red blood cells, respectively. The results indicated that the copper complex (6) did not display any toxicity and haemolysis activity on the healthy cells at concentrations up to 32  $\mu\text{g}/\text{mL}$ .

### 3.3. Inhibitory activity study against *M. tuberculosis H37Rv* strain

The synthesized complexes were screened for their antitubercular potential against *Mycobacterium tuberculosis H37Rv* strain. Isoniazid,

Streptomycin, Rifampin, Pyrazinamide, and Ethambutol were used as standard drugs for comparison of results. Further, the minimum inhibitory concentration (MIC) of the compounds essential for inhibition of  $H_{37Rv}$  growth was calculated. Among all the compounds tested, only vanadium complex (5) showed better activity with MIC comparable with the standard anti-TB drugs (Table 3).

### 3.4. Toxicity studies on HEK cell line

The vanadium complex (5) which was identified as a hit candidate for anti-TB activity, was further evaluated for its cytotoxicity effects on human embryonic kidney cells using MTT Assay. It was found that the compound exhibited a good safety profile for healthy cells with an  $IC_{50}$  value of 5.63  $\mu\text{g}/\text{mL}$ , which is higher than the MIC value of the same

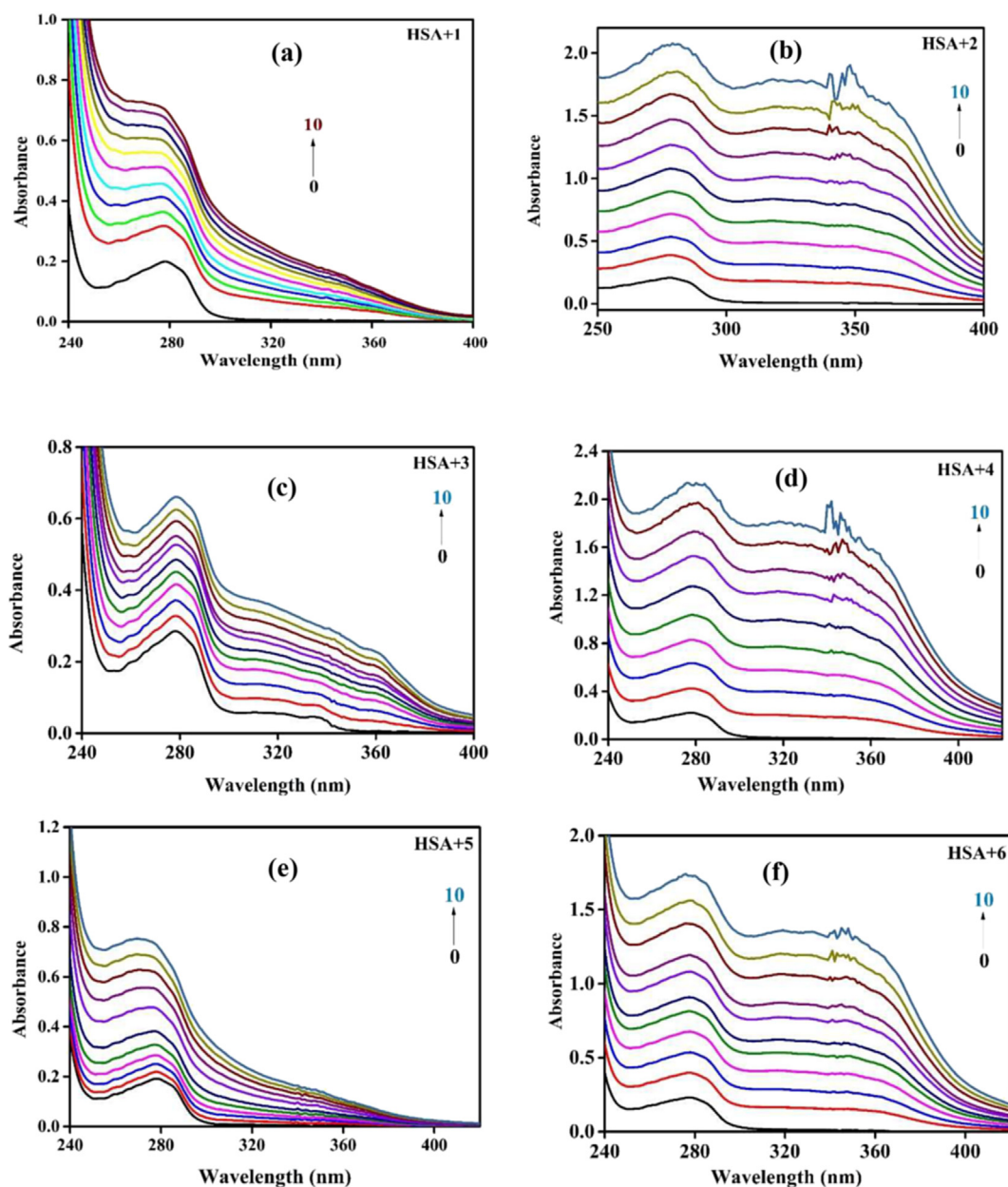


Figure-5. UV-Visible spectrum of HSA upon titration with different concentrations of (a)  $V^VO_2(\text{Quibal-INH})$  (1), (b)  $[Cu^II(\text{Quibal-INH})_2]$  (2), (c)  $[V^VO(\text{Quibal-INH})(cat)]$  (3), (d)  $[Cu^II(\text{Quibal-INH})(cat)]$  (4), (e)  $[V^VO(\text{Quibal-INH})(bha)]$  (5) and (f)  $[Cu^II(\text{Quibal-INH})(bha)]$  (6).

compound. This depicts the non-toxicity of the vanadium complex 5 below its MIC value. Therefore, this compound can be taken for advanced biological/clinical trials.

### 3.5. Free radical scavenging study

All the developed compounds were evaluated for their antioxidant potential with the help of a DPPH radical scavenging assay. The radical scavenging capacity was evaluated by the representative changes in the absorbance at a wavelength of 517 nm for the test solutions of compounds added with DPPH. The scavenging ability of the ligand and complexes were examined by plotting a graph of scavenging effect percentage v/s concentration. The half-maximal effective concentration ( $EC_{50}$ ) of the compounds was determined using the scavenging activity values (Table 4). Standard antioxidant compound ascorbic acid was used for comparison as a reference, whose  $EC_{50}$  value was 66.42  $\mu\text{M}$ . Copper complex 4 exhibited excellent free radical scavenging activity with  $EC_{50}$

value of 18.33  $\mu\text{M}$ , depicting higher activity than ascorbic acid. In addition, the vanadium and copper complexes 5 and 6 also displayed significant antioxidant activity, with  $EC_{50}$  values comparable to that of standard ascorbic acid (Table 4). The scavenging ability of the most active complexes 4, 5 and 6 were examined by plotting a graph of scavenging effect percentage v/s concentration mentioned in Figures 3a, 3b and 3c respectively.

### 3.6. Model biological media interaction effects

#### 3.6.1. pH variation effects

Evaluating the stability of the compounds in varying pH conditions is essential owing to varied biological pH ranging from basic to acidic conditions in the biological drug route. Titration experiments at varied pH using pH meter and UV-visible spectroscopy were done to understand the stability of ligand and its metal complexes in solution. Firstly, the physicochemical parameter  $pK_a$  was found using pH potentiometric

titration experiments. For all the compounds (0.5 mM), the initial solution pH was steadily decreased to about pH 2 by the gradual addition of HCl solution (50 mM). The solutions were then titrated by the gradual addition of KOH solution (50 mM) and a plot of pH v/s volume of KOH used was drawn to calculate the equivalence point and  $pK_a$  values (see Supporting information SI Figure 3, page S7–S10). The  $pK_a$  values ranged from 3.68 to 4.69 for all compounds. Titrations of compounds with acid and base were also studied by measuring UV-Vis absorbance to understand the stability of transition peaks. Acidic and basic pH environments encouraged hypochromism and hyperchromism, respectively but failed to result in any wavelength shift in the peak absorbance (Figure 4). The acceptable values of  $pK_a$  and the retaining peaks of absorbance for the compounds in wide-ranging pH recommend that the complexes possess great potential to bypass the biological drug route and display excellent physiological stability.

### 3.6.2. Protein titration effects

Evaluation of the interaction of a prospective drug with biological proteins is of prime importance. It plays a decisive role in evaluating the drug regimen, toxicity, and bioavailability of the drug candidates. Considering this, the interaction of copper and vanadium complexes with HSA, a model plasma protein, was examined using the UV-Visible spectroscopic technique to gain preliminary insight into their extent of binding [38]. HSA is known to show absorption maxima at 280 nm [39], which forms a key factor in the analysis of the interaction between the test compound and HSA. The UV-Vis spectra of HSA (5  $\mu$ M) with titration of metal complexes (1–6) at varied concentrations (0.83–8.19  $\mu$ M) in pH 7.4 medium at 298 K were studied (Figure 5). It was observed that the intensity of absorbance of HSA increased with incremental concentrations of the complexes, which recommended a static interaction between protein and compounds [40]. To deduce the binding constant  $K_a$  and extent of binding, a double reciprocal plot ( $A_0/(A-A_0)$  vs.  $1/c$ ) acquired from the absorbance data was used, as shown in Supporting information SI Figure 4 page S11–S13. The calculated association constants ( $K_a$ ) were found to be in the range of  $0.062$ – $5.25 \times 10^5$ . The HSA interaction studies infer that in the presence of biological media and plasma the synthesized complexes are quite stable enough; thereby, they can possibly bypass many biological barriers and drug routes. Additionally, plasma proteins like HSA could be explored as transporters of these drug candidate compounds.

## 4. Conclusion

Novel  $V^V$  and  $Cu^{II}$  complexes with ligand Quibal–INH and co-ligands, catechol and BHA, were synthesized and characterized using different analytical and spectroscopic techniques to ascertain the structural and molecular formulae of the complexes. The ligand was found to coordinate in an ON–donor fashion. The therapeutic activities of the coordination compounds were evaluated primarily in terms of their in vitro activities toward high-risk antimicrobial-resistant pathogens and *M. tuberculosis*  $H_{37}R_v$  strain. The complexes were also assessed for their free-radical scavenging potential. The results conclude that all the developed compounds are plausibly bioactive and to specifically highlight,  $[Cu^{II}(\text{Quibal-INH})(\text{bha})]$  (6) displayed growth inhibition of *Candida albicans* and *Cryptococcus neoformans* fungal species with no toxicity and hemolysis activity on the healthy cells at concentrations up to 32  $\mu$ g/mL  $[V^VO(\text{Quibal-INH})(\text{bha})]$  (5) exhibited significant activity against *M. tuberculosis*  $H_{37}R_v$  strain as compared to the standards.  $[Cu^{II}(\text{Quibal-INH})(\text{cat})]$  (4) exhibited excellent free radical scavenging activity higher than the activity of standard ascorbic acid. In addition, the complexes  $[V^VO(\text{Quibal-INH})(\text{bha})]$  (5) and  $[Cu^{II}(\text{Quibal-INH})(\text{bha})]$  (6) also displayed significant antioxidant activity. The synthesized coordination complexes demonstrated stability at physiological conditions of pH and exhibited a high extent of binding with HSA plasma protein signifying effective transport of the new drug-alike candidates in biological conditions.

## Declarations

### Author contribution statement

Anamika Sinha, Riya Chaudhary: Conceived and designed the experiments; Performed the experiments; Wrote the paper. Dinesh S. Reddy, Manasa Kongot: Conceived and designed the experiments; Analyzed and interpreted the data; Wrote the paper. Mahantesh M. Kurjogi: Performed the experiments; Wrote the paper. Amit Kumar: Conceived and designed the experiments; Analyzed and interpreted the data; Contributed reagents, materials, analysis tools or data; Wrote the paper.

### Funding statement

This work was supported by Science and Engineering Research Board (SERB), India [SB/FT/CS-100/2013] and Jain University (Centre for Nano and Material Sciences (CNMS)).

### Data availability statement

Data included in article/supplementary material/referenced in article.

### Declaration of interest

The authors declare no conflict of interest

### Additional information

Supplementary content related to this article has been published online at <https://doi.org/10.1016/j.heliyon.2022.e10125>.

## References

- [1] World Health Organization, Antimicrobial Resistance. <https://www.who.int/news-room/fact-sheets/detail/antimicrobial-resistance> (accessed on 19th Oct, 2021).
- [2] (a) D.S. Reddy, M. Kongot, A. Kumar, Coumarin hybrid derivatives as promising leads to treat tuberculosis: recent developments and critical aspects of structural design to exhibit anti-tubercular activity, *Tuberculosis* 127 (2021), 102050; (b) M. Akki, D.S. Reddy, K.S. Katagi, A. Kumar, H.C. Devarajegowda, S.M. Kumari, V. Babagond, S. Mane, S.D. Joshi, Synthesis of coumarin-thioether conjugates as potential anti-tubercular agents: their molecular docking and X-ray crystal studies, *J. Mol. Struct.* 1266 (2022), 133452; (c) D. Cirri, A. Pratesi, T. Marzo, L. Messori, Metallo therapeutics for COVID-19. Exploiting metal-based compounds for the discovery of new antiviral drugs, *Expert Opin. Drug Discov.* 16 (2021) 39–46.
- [3] (a) D.S. Reddy, A. Sinha, A. Kumar, V.K. Saini, Drug Re-engineering and Repurposing: A Significant and Rapid Approach to Tuberculosis Drug Discovery, *Arch Pharm, Weinheim*, 2022, e2200214; (b) T. Marzo, L. Messori, A role for metal-based drugs in fighting Covid-19 infection? the case of Auranofoin, *ACS Med. Chem. Lett.* 11 (2020) 1067–1068.
- [4] P.J. Loehrer, L.H. Einhorn, Cisplatin, *Ann. Intern. Med.* 100 (1984) 704–713.
- [5] A.W. Prestayko, J. D'aoust, B. Issell, S. Croke, Cisplatin (cis-diamminedichloroplatinum II), *Cancer Treat Rev.* 6 (1979) 17–39.
- [6] A.J. Wagstaff, A. Ward, P. Benfield, R.C. Heel, Carboplatin, *Drugs* 37 (1989) 162–190.
- [7] M.-X. Tan, Z.-F. Wang, Q.-P. Qin, B.-Q. Zou, H. Liang, Complexes of oxoplatin with rhein and ferulic acid ligands as platinum (IV) prodrugs with high anti-tumor activity, *Dalton Trans.* 49 (2020) 1613–1619.
- [8] S. Rafique, M. Idrees, A. Nasim, H. Akbar, A. Athar, Transition metal complexes as potential therapeutic agents, *Biotechnol. Mol. Biol. Rev.* 5 (2010) 38–45.
- [9] K.D. Mjos, C. Orvig, Metallo drugs in medicinal inorganic chemistry, *Chem. Rev.* 114 (2014) 4540–4563.
- [10] J.C. Pessoa, S. Etcheverry, D. Gambino, Vanadium compounds in medicine, *Coord. Chem. Rev.* 301 (2015) 24–48.
- [11] A. Regiel-Futyra, J.M. Dąbrowski, O. Mazuryk, K. Śpięwak, A. Kyzioł, B. Pucelik, M. Brindell, G. Stochel, Bioinorganic antimicrobial strategies in the resistance era, *Coord. Chem. Rev.* 351 (2017) 76–117.
- [12] I. Correia, P. Adao, S. Roy, M. Wahba, C. Matos, M.R. Maurya, F. Marques, F.R. Pavan, C.Q. Leite, F. Aveicella, Hydroxyquinoline derived vanadium (IV and V) and copper (II) complexes as potential anti-tuberculosis and anti-tumor agents, *J. Inorg. Biochem.* 141 (2014) 83–93.
- [13] A.Z. El-Sonbaty, W.H. Mahmoud, G.G. Mohamed, M.A. Diab, S.M. Morgan, S.Y. Abbas, Synthesis, characterization of Schiff base metal complexes and their biological investigation, *Appl. Organomet. Chem.* 33 (2019) e5048.

- [14] A. Sakthivel, B. Thangagiri, N. Raman, J. Joseph, R. Guda, M. Kasula, L. Mitu, Spectroscopic, SOD, anticancer, antimicrobial, molecular docking and DNA binding properties of bioactive VO (IV), Cu (II), Zn (II), Co (II), Mn (II) and Ni (II) complexes obtained from 3-(2-hydroxy-3-methoxybenzylidene) pentane-2, 4-dione, *J. Biomol. Struct. Dyn.* (2020) 1–15.
- [15] S.D. Oladipo, B. Omondi, C. Mocktar, Synthesis and structural studies of nickel (II)- and copper (II)-N, N'-diarylformamidino dithiocarbamate complexes as antimicrobial and antioxidant agents, *Polyhedron* 170 (2019) 712–722.
- [16] S. Bharti, M. Choudhary, B. Mohan, S. Rawat, S. Sharma, K. Ahmad, Syntheses, spectroscopic characterization, SOD-like properties and antibacterial activities of dimer copper (II) and nickel (II) complexes based on imine ligands containing 2-aminothiophenol moiety: X-ray crystal structure determination of disulfide Schiff bases, *J. Mol. Struct.* 1164 (2018) 137–154.
- [17] D.X. West, A.E. Liberta, S.B. Padhye, R.C. Chikate, P.B. Sonawane, A.S. Kumbhar, R.G. Yerande, Thiosemicarbazone complexes of copper (II): structural and biological studies, *Coord. Chem. Rev.* 123 (1993) 49–71.
- [18] B. Bottari, R. Maccari, F. Monforte, R. Ottana, E. Rotondo, M. Vigorita, Isoniazid-related copper (II) and nickel (II) complexes with antimycobacterial in vitro activity. Part 9, *Bioorg. Med. Chem. Lett* 10 (2000) 657–660.
- [19] R. Maccari, R. Ottana, B. Bottari, E. Rotondo, M.G. Vigorita, In vitro advanced antimycobacterial screening of cobalt (II) and copper (II) complexes of fluorinated isonicotinoylhydrazones, *Bioorg. Med. Chem. Lett* 14 (2004) 5731–5733.
- [20] B. Nazirkar, M. Mandewale, R. Yamgar, Synthesis, characterization and antibacterial activity of Cu (II) and Zn (II) complexes of 5-aminobenzofuran-2-carboxylate Schiff base ligands, *Journal of Taibah University for Science* 13 (2019) 440–449.
- [21] H. Kargar, A.A. Ardakani, K.S. Munawar, M. Ashfaq, M.N. Tahir, Nickel (II), copper (II) and zinc (II) complexes containing symmetrical Tetradentate Schiff base ligand derived from 3, 5-diiodosalicylaldehyde: synthesis, characterization, crystal structure and antimicrobial activity, *J. Iran. Chem. Soc.* (2021) 1–11.
- [22] D. Rehder, Vanadium. Its Role for Humans, *Interrelations between Essential Metal Ions and Human Diseases*, 2013, pp. 139–169.
- [23] M. Patel, S. Patel, M. Chhasatia, P. Parmar, Five-coordinated oxovanadium (IV) complexes derived from amino acids and ciprofloxacin: synthesis, spectral, antimicrobial, and DNA interaction approach, *Bioorg. Med. Chem. Lett* 18 (2008) 6494–6500.
- [24] M. Sahani, U. Yadava, O. Pandey, S. Sengupta, Synthesis, spectral characterization and antimicrobial studies of nano-sized oxovanadium (IV) complexes with Schiff bases derived from 5-(phenyl/substituted phenyl)-2-hydrazino-1, 3, 4-thiadiazole and indoline-2, 3-dione, *Spectrochim. Acta Mol. Biomol. Spectrosc.* 125 (2014) 189–194.
- [25] Z.-Q. Sun, S.-F. Yu, X.-L. Xu, X.-Y. Qiu, S.-J. Liu, Two vanadium (V) complexes derived from bromo and chloro-substituted hydrazone ligands: syntheses, crystal structures and antimicrobial property, *Acta Chim. Slov.* 67 (2020) 1281–1289.
- [26] P.I.d.S. Maia, F.R. Pavan, C.Q. Leite, S.S. Lemos, G.F. de Sousa, A.A. Batista, O.R. Nascimento, J. Ellena, E.E. Castellano, E. Niquet, Vanadium complexes with thiosemicarbazones: synthesis, characterization, crystal structures and anti-Mycobacterium tuberculosis activity, *Polyhedron* 28 (2009) 398–406.
- [27] R.A. Rowe, M.M. Jones, *Inorganic Syntheses*, Wiley, New York, USA, 1957.
- [28] M. Kongot, N. Dohare, V. Singh, D.S. Reddy, N.K. Singhal, R. Patel, A. Kumar, A novel biocompatible Ni(II) tethered moiety as a glucose uptake agent and a hit against methicillin-resistant *Staphylococcus aureus*, *Eur. J. Pharmaceut. Sci.* 123 (2018) 335–349.
- [29] (a) M.C. Lourenco, M.V. de Souza, A.C. Pinheiro, M.d.L. Ferreira, R.S. Gonçalves, T.C.M. Nogueira, M.A. Peralta, Evaluation of anti-tubercular activity of nicotinic and isoniazid analogues, *Arkivoc* 15 (2007) 181–191; (b) MTT Cell Proliferation Assay Instruction Guide – ATCC, VA, USA, [www.atcc.org](http://www.atcc.org); (c) D. Gerlier, N. Thomasset, Use of MTT colorimetric assay to measure cell activation, *J. Immunol. Methods* 94 (1986) 57–63.
- [30] (a) A.A. Al-Amieri, A.A.H. Kadhum, A.B. Mohamad, Antifungal and Antioxidant Activities of Pyrrolidone Thiosemicarbazone Complexes, *Bioinorganic Chemistry and Applications*, 2012, p. 2012; (b) O.P. Sharma, T.K. Bhat, DPPH antioxidant assay revisited, *Food Chem.* 113 (2009) 1202–1205.
- [31] (a) M. Kongot, D. Reddy, V. Singh, R. Patel, N.K. Singhal, A. Kumar, Potent drug candidature of an ONS donor tethered copper (II) complex: anticancer activity, cytotoxicity and spectroscopically approached BSA binding studies, *Spectrochim. Acta Mol. Biomol. Spectrosc.* 212 (2019) 330–342; (b) M. Kongot, N. Dohare, D.S. Reddy, N. Pereira, R. Patel, M. Subramanian, A. Kumar, In vitro apoptosis-induction, antiproliferative and BSA binding studies of an oxidovanadium (V) complex, *J. Trace Elem. Med. Biol.* 51 (2019) 176–190; (c) D.S. Reddy, M. Kongot, V. Singh, M.A. Siddiquee, R. Patel, N.K. Singhal, F. Avecilla, A. Kumar, Biscoumarin-pyrimidine conjugates as potent anticancer agents and binding mechanism of hit candidate with human serum albumin, *Arch. Pharm. (Weinheim)* 354 (2021), e2000181.
- [32] (a) D.S. Reddy, M. Kongot, V. Singh, N. Maurya, R. Patel, N.K. Singhal, F. Avecilla, A. Kumar, Coumarin tethered cyclic imides as efficacious glucose uptake agents and investigation of hit candidate to probe its binding mechanism with human serum albumin, *Bioorg. Chem.* 92 (2019), 103212; (b) D.S. Reddy, M. Kongot, S.P. Netalkar, M.M. Kurjogi, R. Kumar, F. Avecilla, A. Kumar, Synthesis and evaluation of novel coumarin-oxime ethers as potential anti-tubercular agents: their DNA cleavage ability and BSA interaction study, *Eur. J. Med. Chem.* 150 (2018) 864–875.
- [33] (a) N. Maurya, M. Parray, J.K. Maurya, A. Kumar, R. Patel, Interaction of promethazine and adiphenine to human hemoglobin: a comparative spectroscopic and computational analysis, *Spectrochim. Acta Mol. Biomol.* 199 (2018) 32–42; (b) B. Aneja, M. Kumari, A. Azam, A. Kumar, M. Abid, R. Patel, Effect of triazoletryptophan hybrid on the conformation stability of bovine serum albumin, *Luminescence* 33 (2018) 464–474.
- [34] (a) D.S. Raja, N.S. Bhuvanesh, K. Natarajan, Effect of N(4)-phenyl substitution in 2-oxo-1,2-dihydroquinoline-3-carbaldehyde semicarbazones on the structure, DNA/protein interaction, and antioxidative and cytotoxic activity of Cu(II) complexes, *Inorg. Chem.* 50 (2011) 12852–12866; (b) J.K. Maurya, A.B. Khan, N. Dohare, A. Ali, A. Kumar, R. Patel, Effect of aromatic amino acids on the surface properties of 1-dodecyl-3-(4-(3-dodecylimidazolidin-1-yl)butyl)imidazolidine bromide gemini surfactant, *J. Disp. Sci. Tech* 39 (2018) 174–180.
- [35] (a) M. Kongot, N. Maurya, N. Dohare, Mud. Parray, J.K. Maurya, A. Kumar, R. Patel, Enthalpy-driven interaction between dihydropyrimidine compound and bovine serum albumin: a spectroscopic and computational approach, *J. Biomol. Struct. Dyn.* 36 (2018) 1161–1170; (b) T. Mukherjee, J.C. Pessoa, A. Kumar, A.R. Sarkar, Formation of an unusual pyridoxal derivative: characterization of Cu(II), Ni(II) and Zn(II) complexes and evaluation of binding to DNA and to human serum albumin, *Inorg. Chim. Acta.* 426 (2015) 150–159.
- [36] J. Peisach, W. Blumberg, Structural implications derived from the analysis of electron paramagnetic resonance spectra of natural and artificial copper proteins, *Arch. Biochem. Biophys.* 165 (1974) 691–708.
- [37] U. Sakaguchi, A.W. Addison, Spectroscopic and redox studies of some copper (II) complexes with biomimetic donor atoms: implications for protein copper centres, *J. Chem. Soc., Dalton Trans.* (1979) 600–608.
- [38] X. Pan, R. Liu, P. Qin, L. Wang, X. Zhao, Spectroscopic studies on the interaction of acid yellow with bovine serum albumin, *J. Lumin.* 130 (2010) 611–617.
- [39] C. Jash, G.S. Kumar, Binding of alkaloids berberine, palmatine and coralyne to lysozyme: a combined structural and thermodynamic study, *RSC Adv.* 4 (2014) 12514–12525.
- [40] K. Das, S. Sanwlani, K. Rawat, C.R. Haughn, M.F. Doty, H. Bohidar, Spectroscopic profile of surfactant functionalized CdSe quantum dots and their interaction with globular plasma protein BSA, *Colloids Surf. A Physicochem. Eng. Asp.* 506 (2016) 495–506.